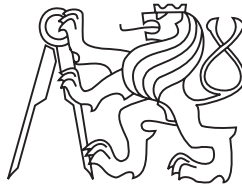


Czech Technical University in Prague
Faculty of Nuclear Sciences and Physical Engineering

Department of Physics



Virtual model of tokamak GOLEM with a real
physical core

BACHELOR THESIS

Author: Martin Matušů
Supervisor: Ing. Vojtěch Svoboda, CSc.
Year: 2014

Insert ASSIGNMENT here.

Prohlášení

Prohlašuji, že jsem svou bakalářskou práci vypracoval samostatně a použil jsem pouze podklady (literaturu, projekty, SW atd.) uvedené v příloženém seznamu.

Nemám závažný důvod proti použití tohoto školního díla ve smyslu § 60 Zákona č.121/2000 Sb., o právu autorském, o právech souvisejících s právem autorským a o změně některých zákonů (autorský zákon).

V Praze dne

.....
Martin Matušů

Poděkování

Děkuji Ing. Vojtěchu Svobodovi, CSc. za vedení mé bakalářské práce a za podnětné návrhy, které ji obohatily a podnítily mé zapálení do oboru. Děkuji také svým blízkým za oporu kterou jsem v nich při práci našel.

Martin Matušů

Název práce:

Virtuální model tokamaku GOLEM s reálným fyzikálním jádrem

Autor: Martin Matušů

Obor: Physics and Technology of Thermonuclear Fusion

Druh práce: Bakalářská práce

Vedoucí práce: Ing. Vojtěch Svoboda, CSc.
Department of Physics, Faculty of Nuclear Sciences and Physical Engineering, Czech Technical University in Prague

Konzultant: prof. Ing. Jiří Žára, CSc.
Katedra počítačové grafiky a interakce, Fakulta elektrotechnická, Czech Technical University in Prague

Abstrakt: Termojaderná fúze je potenciálním zdrojem energie na další staletí. Pro její dosažení je třeba napodobit podmínky v centru Slunce. Za těchto podmínek je však všechna hmota v plazmatickém skupenství. K vytvoření prostředí umožňujícího vznik plazmatu je třeba termojaderného reaktoru. Požadavky na takovýto reaktor jsou shrnuty do Lawsonova kritéria. Jeho splnění se mimo jiné blíží zařízení tokamak. Za využití silného uzavřeného magnetického pole je plasma udrženo v komoře tokamaku. Takové uspořádání však s sebou nese technickou náročnost experimentu. Pro testování materiálů a diagnostik byla postavena řada menších tokamaků, v nichž není možné udržet termojadernou fúzi. Jedním z nich je i tokamak GOLEM sloužící jako výukové zařízení na Fakultě jaderné a fyzikálně inženýrské Českého vysokého učení technického v Praze. Jednou z nejdůležitějších vlastností tohoto tokamaku je možnost řízení výbojů vzdáleně pomocí webového rozhraní. Toto zaměření dalo důvod k vytvoření virtuálního modelu umožňujícího přiblížení reálného tokamaku. Aby byl model jednoduše dostupný a prezentovatelný, bylo opět zvoleno internetové prostředí. K umístění grafických prvků modelu na web byla použita knihovna WebGL. Na takto vytvořený model bylo navázáno jádro fyzikálních simulací reflektujících se v grafickém modelu. Celý model je přístupný na serveru tokamaku GOLEM na adrese: <http://golem.fjfi.cvut.cz/virtual/matusu/BachelorThMM/BMM.html>

Klíčová slova: Termojaderná fúze, Fyzika plazmatu, Tokamak, 3D grafika, WebGL, Online prezentace

Title:

Virtual model of tokamak GOLEM with a real physical core

Author: Martin Matusů

Abstract:

Thermonuclear fusion is a potential energy source for next few centuries. In order to control this process on Earth, it is necessary to simulate conditions of Sun core. All matter is in plasma state in these conditions and therefore a thermonuclear reactor is needed to create a environment for the plasma. Requirements on such a reactor are stated in Lawson criterion. Tokamak device is except other types of thermonuclear reactor close to meet Lawson criterion. This device uses a strong closed magnetic field to confine plasma within reactor vessel. On the other hand, this set-up brings technical difficulties of the whole experiment. A lot of small tokamaks, which cannot meet fusion conditions, were build for a purpose of material and diagnostics testing. One of them is a GOLEM tokamak operating as an educational device at the Faculty of Nuclear Sciences and Physical Engineering of the Czech Technical University in Prague. One of the most important functions of this tokamak is a discharge remote control via web interface. This specification set the main idea of a creation of a virtual model, which would give user more specific conception of the real tokamak. In order to make the model easy accessible, internet environment has been chosen again. Graphical elements of model were placed on the web with the use of a library WebGL. Such a model was extended by a physical core of simulations, reflecting back at the graphical model. The whole program is accessible on the GOLEM server at: <http://golem.fjfi.cvut.cz/virtual/matusu/BachelorThMM/BMM.html>

Key words:

Thermonuclear fusion, Plasma physics, Tokamak, 3D grafics, WebGL, Online presentation

Contents

Introduction	8
1 Thermonuclear fusion	9
1.1 Principle	9
1.2 Plasma	11
1.3 Lawson criterion	13
1.4 Approaches to fusion	15
2 Tokamak	16
2.1 Basic principles of tokamak technology	17
2.2 Toroidal magnetic field \mathbf{B}_t	19
2.3 The GOLEM tokamak	22
2.3.1 Setup	22
2.3.2 Diagnostics	24
2.3.3 GOLEM strategy	25
3 Virtual model	26
3.1 Programming of online graphics	27
3.2 The environment and other functions of the model	28
3.2.1 Project vision	29
3.3 Capacitor curve	33
3.4 Models of the toroidal magnetic field \mathbf{B}_t	34
Summary	39
Bibliography	40
Appendix	42
A Table of variables	43

Introduction

World energy needs and nuclear power

Considering the speed of the growth of energy needs, humanity has to figure out how to solve this issue in the long term horizon. For a long time, burning fossil fuels has been a sufficient method to cover energy demands. But this method has two main problems, the scarcity of fuel and ecological consequences. The Manhattan project provided an alternative which was not essentially burdened by previous problems. But with the occurrence of accidents in fission power plants and a still growing energy demand, another source of energy is needed. With advanced knowledge of physics it may appear that renewable energy is the best way to solve this crisis. Although renewable energy may be the final solution of energetics problem of humanity, the technology to achieve this utopia is not sufficiently developed. Therefore there is a need to find a solution in this current period. A convenient source of energy has been found by understanding the Sun. In its centre, an enormous amount of energy is generated due to the process of fusion.

Chapter 1

Thermonuclear fusion

1.1 Principle

Nuclear fusion is a process in which two or more light atomic nuclei collide and join to form a more complicated nucleus. A mass analysis of the reaction participants leads to a fascinating result, that the mass of the more complicated nucleus will be less than the sum of the masses of the individual nuclei. This results in an energy yield E according to Einstein's equation for the difference Δm in the masses of the reactants and the products of the reaction

$$E = \Delta mc^2, \tag{1.1}$$

where c stands for the speed of light.

The greatest difficulty of nuclear fusion is the electric force given by Coulomb's law. It postulates a force in a direction dependent on the charges polarity of the considered bodies and is inversely proportional to the square of the distance between them. Thus with positively charged nuclei, the repulsive electric force creates a potential barrier that has to be overcome. If there was only Coulomb's force, this barrier would be infinite and fusion would be impossible. Real nuclear synthesis is enabled by the existence of another fundamental force, a strong interaction, which is about a hundred times stronger than the electromagnetic interaction, but its range is in the order of femtometres. With a rising nucleon number, the strong force per particle increases and the nucleus becomes more stable. But the growth of stability stops at the point, where the diameter of the nucleus overreaches the effective distance of strong interaction. Elements with a spacious nucleus are again less stable and may release energy by the fission. Although this energy seems greater than the energy released by fusion, the energy per nucleus is a few times smaller (see graph 1.1). These two forces together create a finite barrier that is overcome in the process of fusion.

This theory claims a finite barrier, though it was too high to explain a model of the Sun

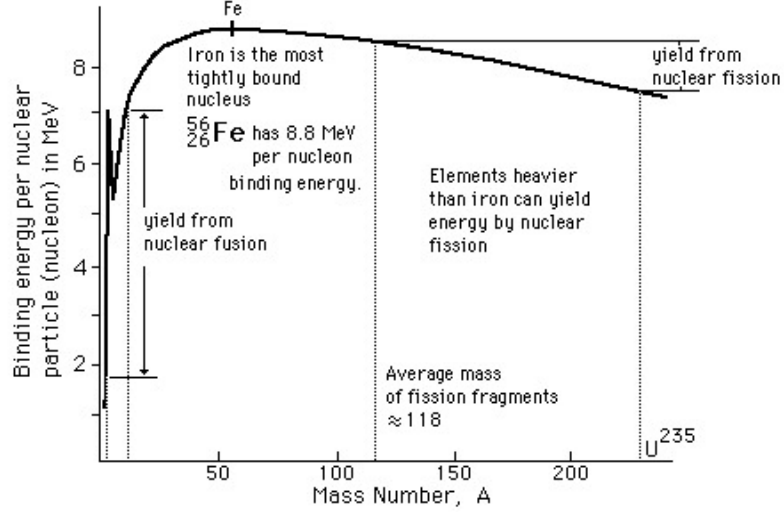


Figure 1.1: The stability of elements; reprinted from [1].

in the early twentieth century. A breakthrough in this field was made by George Gamow, who explained alpha decay by quantum tunnelling. With knowledge of this phenomenon, models of the Sun were recalculated and corresponded with observations of this star.

Gamow derived [2, 1.56] a formula 1.2, that can be used to calculate the necessary energy of the nuclei, whose proton numbers are Z_1 and Z_2 and their reduced mass μ , to be fused.

$$\langle \sigma v_r \rangle = \frac{8}{\sqrt{3}} \frac{\hbar}{\pi e^2 Z_1 Z_2 \mu} \xi^2 S_0 \exp(-3\xi) \quad (1.2)$$

In this formula $\langle \sigma v_r \rangle$ is the reaction rate, function $\xi \sim T^{-\frac{1}{3}}$, S_0 is called the astrophysical S factor and is a weak function of the center of mass energy of the reaction. Even with quantum tunnelling, equation 1.2 results in an ideal energy of 64 keV of the nuclei in the centre of the mass coordinates for a deuterium-tritium fusion (D-T) reaction [2, p.12]. Nuclei with this energy have highest probability of tunnelling through the barrier and fusing.

There are several ways to overcome the barrier in order to make nuclei fuse. Except for cold fusion and muon catalysed fusion, which are not issues of this work, all methods assume the energy of particles from the heat. The ideal temperature of matter for D-T fusion is approximately 30 keV, which is an equivalent of 300 million kelvins. At these values, all matter is in a plasma state. Therefore, in order to understand the conditions of thermonuclear fusion, it is necessary to study plasma physics.

1.2 Plasma

“Plasma is a quasi-neutral gas of charged and neutral particles, which shows collective behaviour.”

-Francis F. Chen, [3, p.19]

Looking closer at this definition, there are two important points: quasi-neutrality and collective behaviour. The meaning of this expression is in more detail described and rewritten in following three conditions:

1. Plasma range

Because the particles in plasma are charged, any segregation of electrons from ions converts their kinetic energy into electrostatic potential. This depends on density n_e of displaced electrons and the volume of displaced electrons, specially in the 2D approximation width Δ of the electron layer. The maximum width, when the layer is displaced by its own width and all kinetic energy E_k is converted into the potential $U_p = -eE\Delta$ because of this displacement, is named the Debye length λ_D . While kinetic energy may be expanded as a product of Boltzmann's constant k_B and the electron temperature T_e , the potential energy is an integral of the electric force eE over the distance λ_D . By consideration of the displaced layer as a 2D capacitor of thickness λ_D , the electric field E fulfils equation 1.3.

$$E = -en_e\lambda_D/\epsilon_0 \quad (1.3)$$

Summing up, the equality of these energies concludes in definition 1.4.

$$\max \Delta = \lambda_D = \left(\frac{\epsilon_0 k_B T_e}{n_e e^2} \right)^{\frac{1}{2}}. \quad (1.4)$$

This length is used in the description of quasi-neutrality. It is the distance, at which the charges in the plasma remains unshielded by other charges. Therefore the whole plasma is neutral, but within a sphere around the charge with this radius, Coulomb force is essential. The first condition of plasma has to be therefore set, so that Debye length has to be much smaller than system size: $L \gg \lambda_D$.

2. Dominance of EM force

The quasi-neutrality term is not valid with quick processes because of the short duration of the mentioned dislocation. In the case of the capacitor described above, dislocation of negative charge with respect to positive background initiates harmonic oscillations with the plasma frequency ω_{pe} . It is possible to describe this electron

displacement Δ as an equation of motion, where electrons with the mass m_e and the charge density en_e experience a restoring force eE created by the electric field 1.3,

$$m_e \frac{d^2 \Delta}{dt^2} = -\frac{e^2 n_e}{\epsilon_0} \Delta, \quad (1.5)$$

where ϵ_0 is the vacuum permittivity. 1.5 is an equation of a harmonic oscillator with a characteristic frequency

$$\omega_{pe} = \left(\frac{n_e e^2}{\epsilon_0 m_e} \right)^{\frac{1}{2}}. \quad (1.6)$$

This variable is called the characteristic plasma oscillation frequency. In order to call a ionised gas a plasma, the electromagnetic force has to be dominant over collisions with neutral particles. If the average time between these collisions is τ_{col} , there has to be fulfilled the condition $\tau_{col} \omega_{pe} > 1$. This condition describes whether a gas acts as plasma or as a neutral gas, [3, p.26].

3. Plasma parameter

To further describe plasma in which collective behaviour dominates binary collision it is necessary to realize, that distant particles affect charged particle much less in comparison with adjacent ones. This phenomenon is called Debye shielding and considers λ_D great enough to contain a lot of particles in its sphere independently of electron density. This condition is formulated by plasma parameter N_D in 1.7.

$$N_D = \frac{4\pi}{3} \lambda_D^3 n_e \gg 1. \quad (1.7)$$

Because this definition is quite general, plasma may occur in different forms. Its density may differ by thirty orders of magnitude and temperature by ten orders of magnitude (see figure 1.2). From this figure should be pointed out Sun's core, whose principle have scientists tried to explain for many centuries, and Tokamaks with Inertial confined fusion (ICF), methods to simulate equivalent conditions on Earth, already standing just next to it.

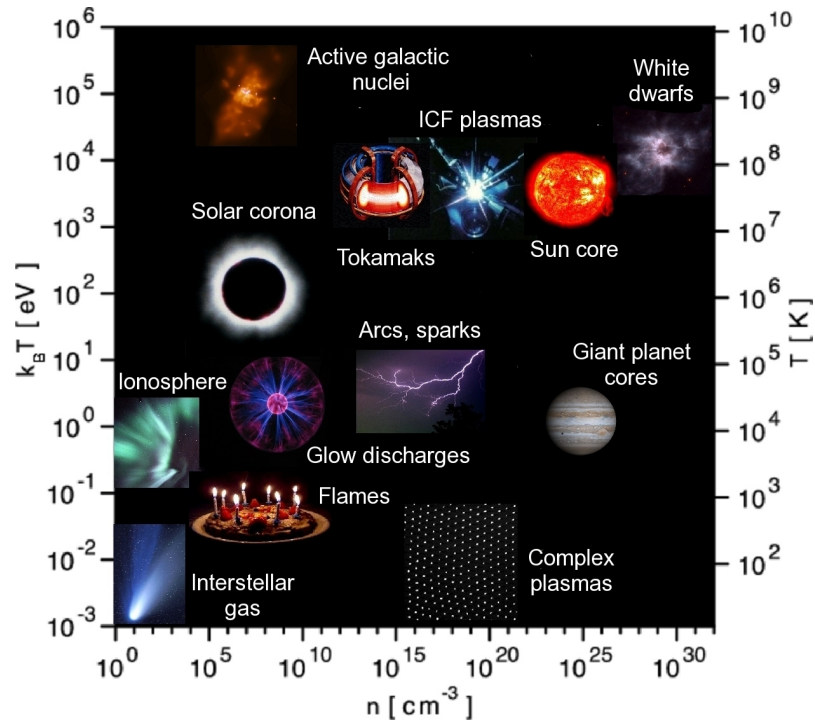


Figure 1.2: Forms of plasma: n stands for density, $E = k_B T$ is energy and T its temperature equivalent; reprinted from [4].

1.3 Lawson criterion

No matter what way of reaching fusion conditions is chosen, it is necessary to consider, if this method can be used as the principle of a fusion power plant. These ideas have been generalized by J.D.Lawson in 1957 as the Lawson criterion. He defined a variable called the confinement time τ_E , mapping the quality of the plasma heat confinement

$$\tau_E = \frac{W_P}{P_L}, \quad (1.8)$$

where the power losses P_L are losses of plasma energy W_P per its volume, compensated by the heating P_H . This relation may be written as

$$P_L = P_H - \frac{dW_P}{dt}. \quad (1.9)$$

Furthermore, the heat power may be rewritten as an addition of the power of external

heating P_e and the captured energy from fusion itself, internal heating P_i .

$$P_H = P_e + P_i \quad (1.10)$$

A very important parameter of a tokamak is fusion gain

$$Q = \frac{P_f}{P_e}, \quad (1.11)$$

which comprises how profitable the method is with a certain fuel. Fusion power P_f is of course dependent on the volume of the plasma V_p , energy gain from one reaction ε_f and the rate of fusion reactions in this volume R_V . This rate is a multiplication of fuel densities and the average of the cross section and relative velocity $\langle \sigma v_r \rangle$, for the D-T reaction

$$P_f = R_V V_p \varepsilon_f = n_D n_T \langle \sigma v_r \rangle V_p \varepsilon_f. \quad (1.12)$$

It is important to realise that part of fusion power is captured by plasma, in D-T reactions alpha particles. Because of action and reaction law, this particle has one fifth of released energy. This energy source is internal power P_i mentioned above. Also plasma energy has its theoretical description. Considering the equipartition theorem, the plasma power W_p may be evaluated 1.13, especially when fuel densities are equal ($n_D = n_T = n/2$)

$$W_p = 3N_p k_B T = 3(n_D + n_T) V_p k_B T = 3n V_p k_B T. \quad (1.13)$$

Since all the variables in 1.8 were restated, it is convenient to study this definition under various conditions. The first apparent condition is plasma without external heating. This condition is called ignition and fusion gain soars to infinity, $Q \rightarrow \infty$. In this condition all that is left to compensate for power losses is the internal power, which even has to exceed the power losses in a useful reactor.

These thoughts brought us to a final version of the Lawson criterion for a useful fusion reactor.

$$\tau_E \geq \frac{W_p}{P_i} = \frac{15n V_p k_B T}{V_p R_V \varepsilon_f} = \frac{60k_B T}{n \langle \sigma v_r \rangle \varepsilon_f}. \quad (1.14)$$

A more useful way of formulating the mentioned criterion is to substitute all the variables dependent on temperature as single function $f_L(T)$.

$$\tau_E n \geq f_L(T). \quad (1.15)$$

In this form, the Lawson criterion also shows the temperature, at which fulfilment of this criterion is most likely to be achieved. For the D-T reaction, this function reaches its minimum at the temperature $T = 30$ keV, [5, p.90].

1.4 Approaches to fusion

In order to obtain these fusion conditions, it is necessary to create a device, which would keep the density n with a rising temperature T high enough to fulfil the Lawson criterion. The cold war brought a diversity of possible solutions. Where the USA developed stellarators, the USSR focused on tokamaks, [6].



Figure 1.3: Model of stellarator coils; reprinted from [7].

Meanwhile, Great Britain started research on pinch devices. These three classical confinement methods all create the necessary conditions with a closed magnetic field. Although open field configurations have been developed too, their energy gain is low and thus cannot be used as a power plant. Later on, when lasers were strong enough, the idea of inertial fusion appeared. This approach may be used in future as a research method, but nowadays unlikely as an energy source due to its high driver energy consumption. On the other hand, magnetic confinement methods have made significant progress in last fifty years and are accepted as a possible way out of an energy crisis. Although both, stellarators and pinches, made significant scientific discoveries, they cannot match tokamaks on the field of confinement time. Even with densities taken in consideration, tokamaks are the closest of them to the fulfilment of the Lawson criterion and therefore are accepted as the most probable principle of a fusion power plant.

Chapter 2

Tokamak

The first idea of the tokamak appeared around 1950 in the USSR. It was O.A.Lavrentev, who wrote a letter to Moscow, including the idea of the electrostatic confinement of deuterium nuclei for the industrial scale generation of energy. His idea was to use two spherical grids under negative and positive potentials for this purpose [6, p.837]. A.Sacharov and I.Tamm improved the whole idea by using a toroidal chamber and by using a magnetic field. This confinement method was simply named “TOroidnaja KAMERA s MAGnitnymi Katuškami” in Russian, which stands for a toroidal chamber with magnetic coils.

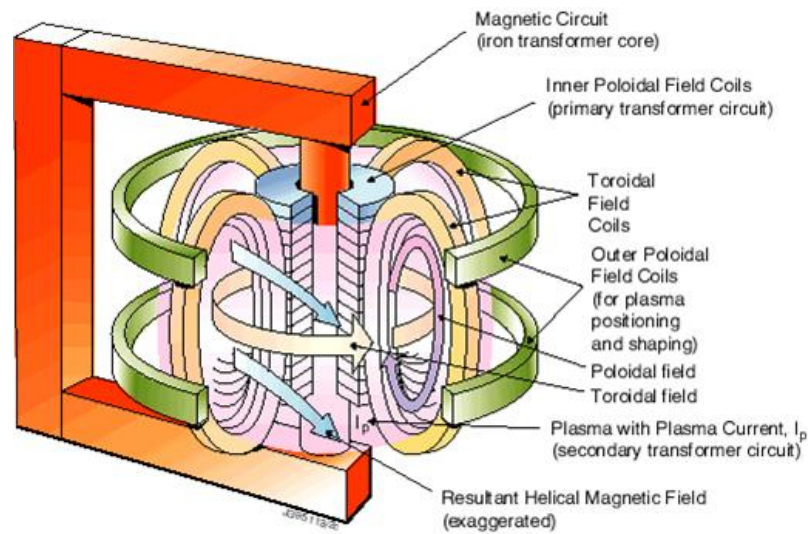


Figure 2.1: The basic principle of the tokamak magnetic field; reprinted from [8].

2.1 Basic principles of tokamak technology

Sacharov's idea uses a set of coils to approximate a magnetic field, which would be created by a solenoid of a toroidal shape, further on called a toroidal magnetic field \mathbf{B}_t . This field is shown among other components of the magnetic field \mathbf{B} inside a tokamak chamber in figure 2.1.

Because the magnetic component of the Lorentz force

$$\mathbf{F}_L = q\mathbf{v} \times \mathbf{B}. \quad (2.1)$$

causes particles with a charge q and a velocity \mathbf{v} to rotate around the magnetic lines, a toroidal magnetic field B_t prevents them from escaping the tokamak as it is a closed magnetic field. But there are many phenomena that disrupt this idea. One of them is $\mathbf{E} \times \mathbf{B}$ drift shown in figure 2.2.

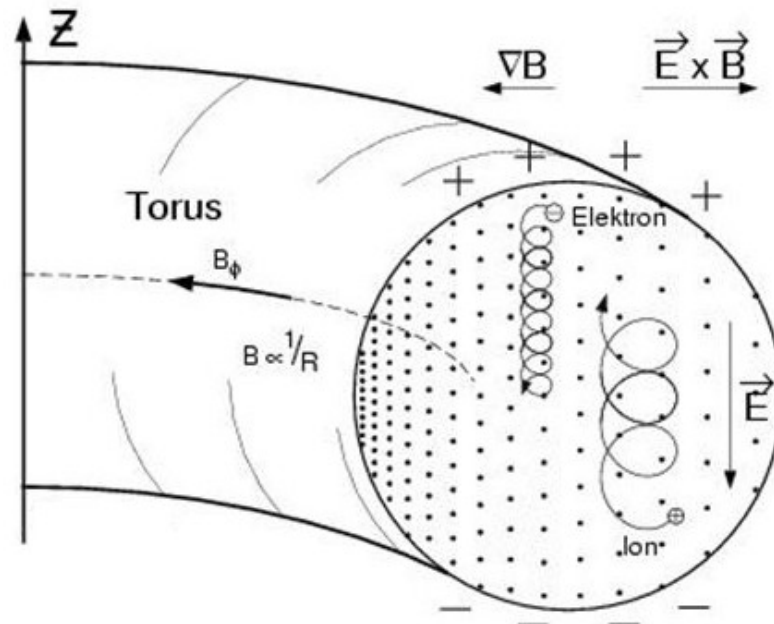


Figure 2.2: $\mathbf{E} \times \mathbf{B}$ drift along the axis of the tokamak vessel; reprinted from [9].

It is a consequence of ∇B , which is derived later in chapter 2.2: Toroidal magnetic field \mathbf{B}_t . The direction of this drift caused by this gradient is along the symmetry axis of the tokamak vessel, top or bottom depending on the charge of the particle. This drift causes a polarity of the plasma and the electric field \mathbf{E}_d . The resulting $\mathbf{E}_d \times \mathbf{B}_t$ drift

is towards the outer wall of the tokamak chamber. In order to compensate this drift, another magnetic field B_p has to be added. It is called a poloidal magnetic field and is perpendicular to the toroidal one (see figure 2.1). Superposition of these magnetic fields results in a helical field

$$\mathbf{B} = \mathbf{B}_p + \mathbf{B}_t, \quad (2.2)$$

which leads to global compensation of drift, as particles follow helical lines. Although Sacharov's first idea was to suspend an additional poloidal situated coil inside the chamber [6, p.839], he realised, that plasma itself may serve as well. To create the necessary current in the plasma, there is a need to drive a current in a toroidal direction. Faraday's law of electromagnetic induction is a great way to achieve this. It postulates induced voltage ϵ_{ind} in an closed electric circuit, e.g., plasma ring, as a result of the time rate of change of the magnetic flux Φ_{tor} through the area enclosed by the circuit, e.g., toroid of the plasma. Moreover, the magnetic flux may be expressed as an integral of the magnetic induction \mathbf{B}_{tor} over the same area.

$$\epsilon_{ind} = -\frac{d\Phi_{tor}}{dt} = -\frac{d}{dt} \int_{S_{tor}} \mathbf{B}_{tor} \cdot d\mathbf{S}. \quad (2.3)$$

Therefore, the whole chamber is embraced by the core of the transformer with a primary winding on it, see figure 2.1. The second winding of transformer is the plasma itself, working as a coil with only one loop.

In general, the magnetic field 2.2 keeps particles from leaving the toroidal shape within the coils. But in order to meet the conditions mentioned in chapter 1.3 Lawson criterion, it is necessary to operate with the work gas only. For this purpose, the tokamak vacuum vessel of a toroidal shape lies within the coils. Moreover, it protects the coils from heat damage caused by hot plasma disturbances.

In such conditions the preparation of the discharge can finally begin. Such preparation consists of three phases:

- At first, it is necessary to drain all the air and reach a high vacuum, so there is almost no contamination in chamber.
- As a proper quality of vacuum is reached, the whole vessel is filled with a working gas, e.g. hydrogen.
- Such a working gas is pre-ionised in order to be affected by the electric field created by the transformer.

Pre-ionisation is not necessary for some ways of reaching a plasma state (RF plasma), but it is the most common way of plasma breakdown assistance. As the working gas is ionised and therefore becomes a closed conductor, the current I_p in orders of MA is induced in the plasma ring by the transformer. Thanks to the Joule effect, the plasma

reaches high temperatures only from this initial electric field. But high temperature of the plasma has an important drawback, i.e. radiation. Such radiation energy losses cannot be suppressed, but have to be compensated for, as they lower the plasma energy. There are a few ways to warm plasma up more, two standing out among others. The first is emitting of electromagnetic waves into the plasma on specific frequencies. Waves at these frequencies are absorbed by the plasma and it is thus heated. The second way is also a method to supply the plasma with fuel, once the plasma particles begin to fuse. By aiming a beam of neutral particles into the plasma. These two ways are needed until the ignition condition $Q \rightarrow \infty$ is reached. Once the plasma meets the conditions to fuse, it compensates its losses by capturing high energy alpha particles from the reaction.

Ever since the working gas reaches high temperatures, it has to be confined by magnetic field 2.2. The whole experiment has to be therefore well timed as the current drive has to be run with toroidal magnetic field \mathbf{B}_t simultaneously to create helical magnetic field.

2.2 Toroidal magnetic field \mathbf{B}_t

The electric current in straight solenoid generates a magnetic field, that is homogeneous within this solenoid. But twisting such a solenoid in a toroid causes some interesting changes. A simple characteristic may be derived with the use of Ampère's circuital law

$$\text{rot}\mathbf{B} = \mu_0\mathbf{j}, \quad (2.4)$$

where \mathbf{j} stands for current density and μ_0 is the permeability of a vacuum. Integrating both sides of the equation over a surface S enclosed by a curve C_i (see figure 2.3, showing the tokamak from above) and the use of Stokes' theorem, it is possible to obtain the set of equations

$$\begin{aligned} \int_S \text{rot}\mathbf{B}_t dS &= \oint_{C_i} \mathbf{B}_t \cdot d\mathbf{l} = 2\pi R B_t, \\ \int_S \mu_0\mathbf{j} dS &= \mu_0 I, \end{aligned} \quad (2.5)$$

resulting in

$$B_t = \frac{\mu_0 I}{2\pi R}, \quad (2.6)$$

where I is the current flowing through the surface S , R stands for the radius from the tokamak axis. This result is dependent on the surface of integration. If there is no current flowing through the surface as it is in the case of the surrounding curve C_1 , the intensity of the toroidal magnetic field is equal to zero.

By extension of the surface to the border C_2 , the current I_{TCF} in the coils is included in the integration surface and thus equation 2.6 describes the toroidal magnetic field B_t

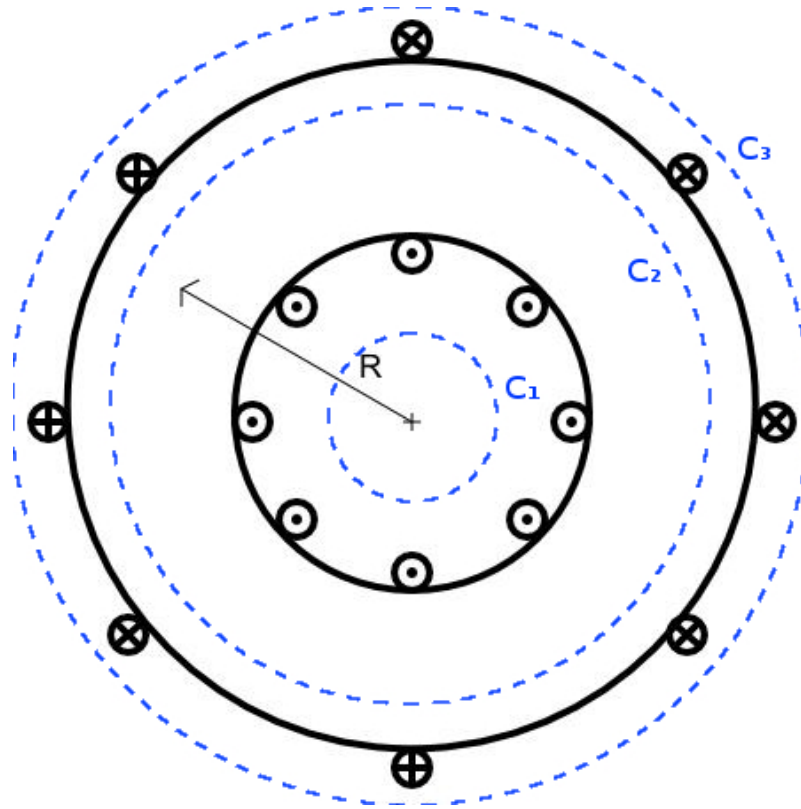


Figure 2.3: Significant border curves C_1 , C_2 and C_3 of the surface S in the derivation of toroidal magnetic field dependency on radius; reprinted from [8].

in dependency on the inverse value of the radius from tokamak axis, [8]. This is a very important knowledge, because it causes some problems, but it may be used in advance too. The dependency of $B_t \sim R^{-1}$ leads to terminology of the high field side (HFS) by the wall of the tokamak closer to the axis of the device and by opposite wall the low field side (LFS). This dependency is shown in figure 2.4.

The third case includes the current in the coils in both directions and the toroidal component of the magnetic field is therefore nullified again.

Derivation by the use of Ampère's circuital law 2.4 shows the basic characteristic of the toroidal magnetic field B_t , but neglects any details of the real situation. As toroidal coils are just an approximation of a continuous solenoid, the magnetic field between each pair of adjacent coils weakens and is stronger close to these coils. This phenomenon is called a ripple in the magnetic field. In order to include this ripple, as well as the dependency on the inverse radius $B_t \sim R^{-1}$, it is possible to create a model based on

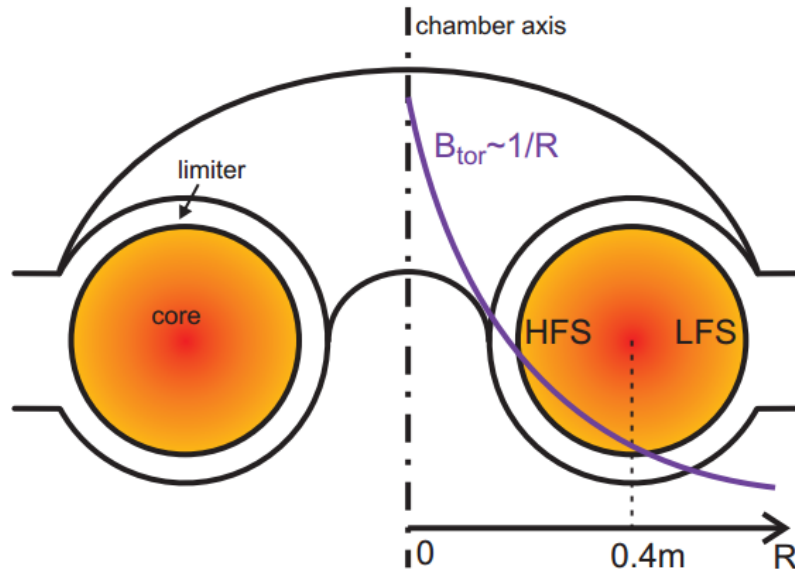


Figure 2.4: The decrease of the toroidal component of the magnetic field $B_t \sim R^{-1}$; reprinted from [10].

the fundamental law of electromagnetism, the Biot-Savart law. This law describes the magnetic field \mathbf{B} at the position \mathbf{r} generated by a steady current I in a conductor described by the path C_{BS} .

$$\mathbf{B} = \frac{\mu_0}{4\pi} \int_{C_{BS}} \frac{I d\mathbf{l} \times \mathbf{r}}{|\mathbf{r}|^3} \quad (2.7)$$

The general use of this law is shown in figure 2.5.

This law allows the calculation of a toroidal magnetic field in any position within the tokamak by simply integrating along the coil, which is in most cases circular, multiplying by the number of turns N as the same current flows through each turn. This has to be done for each coil in order to obtain the vector of magnetic induction in a chosen position. Of course, it is possible to use the axis symmetry of the tokamak again when the grid of positions is chosen wisely. This easement is described in more detail in chapter 3:Virtual model and shown on a specific numerical model. This numerical model is calculated for the GOLEM tokamak, the oldest still operational tokamak, working as an educational device at the faculty for domestic as well as for foreign students.

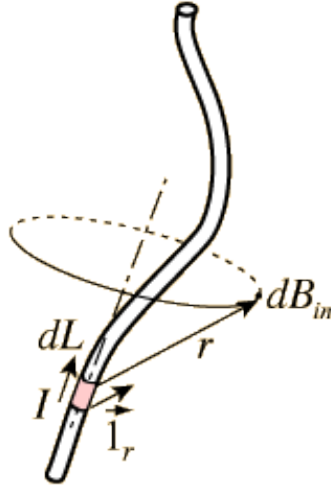


Figure 2.5: The Biot-Savart law describing the magnetic field B in the position r ; reprinted from [11].

2.3 The GOLEM tokamak

This originally soviet device the TM-1 was developed with the purpose of testing the first external heating by a microwave gun. It was moved to Prague and started its work under the designation CASTOR in 1977. Later, when the Institute of Plasma Physics of the Czech Academy of Sciences in the Czech Republic gained the COMPASS tokamak from England, GOLEM was given to the Faculty of Nuclear Sciences and Physical Engineering, where it remains today, [12].

2.3.1 Setup

GOLEM is classified as a small tokamak for its chamber of circular cross-section with a minor radius of $r_0=0.1$ m and a major radius of $R_0=0.4$ m. Its plasma with current $I_p \sim 10^3$ A is confined by a toroidal magnetic field $B_t \sim 3 \cdot 10^{-1}$ T, which is generated by 28 poloidal oriented coils. These coils energy supply is granted by capacitor banks with a total capacitance of $C_B = 67.5$ mF. In these conditions plasma is generated for an average discharge time of $\tau \sim 10^{-2}$ s and reaching an electron temperature of $T_e \sim 40$ eV.

As may be seen from the engineering schematic in figure 2.6, the iron core of transformer is implemented into the plasma current drive system. The schematic also depicts all the main systems of operation and their power supply provided by capacitor banks. These capacitor banks, with a total capacitance of $C_G = 81$ mF, are charged from the public

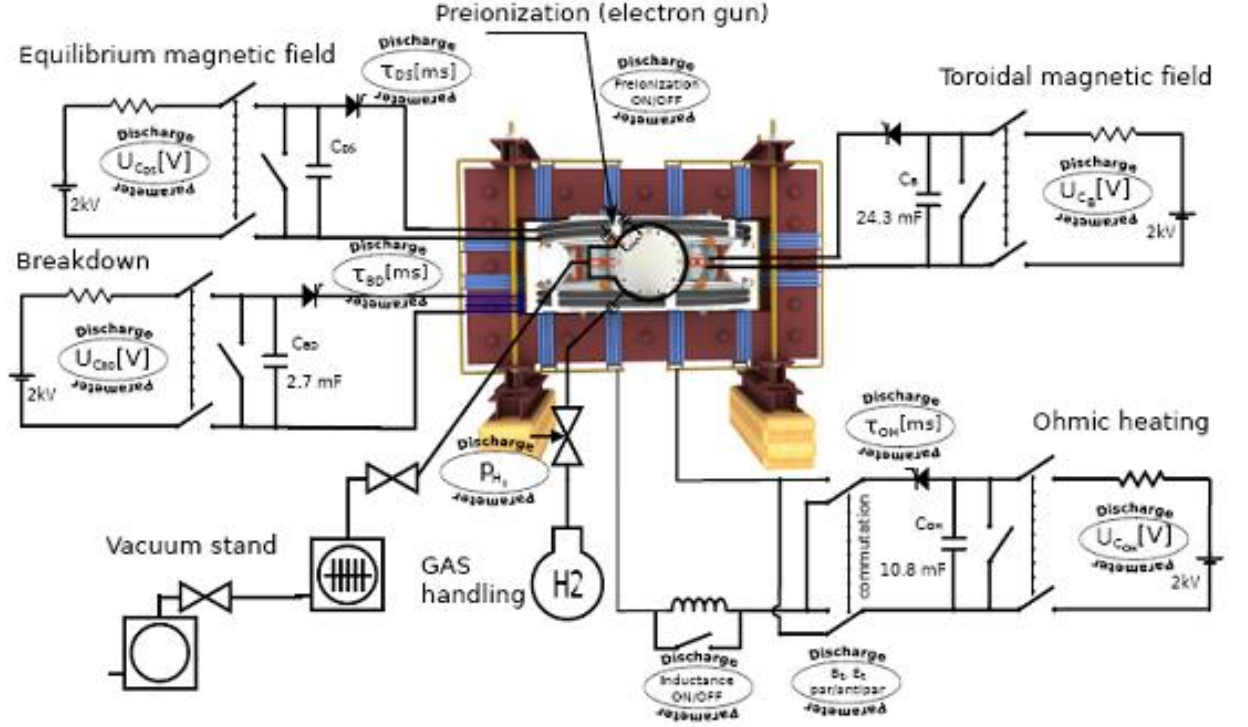


Figure 2.6: Engineering schematic of the GOLEM tokamak, describing its main systems; reprinted from [13].

power network by the supply voltage changed to a value of $\epsilon = 850$ V. Electrostatics derives a formula for capacitor charging

$$U(t) = \epsilon \left[1 - \exp\left(-\frac{t}{R_C C}\right) \right], \quad (2.8)$$

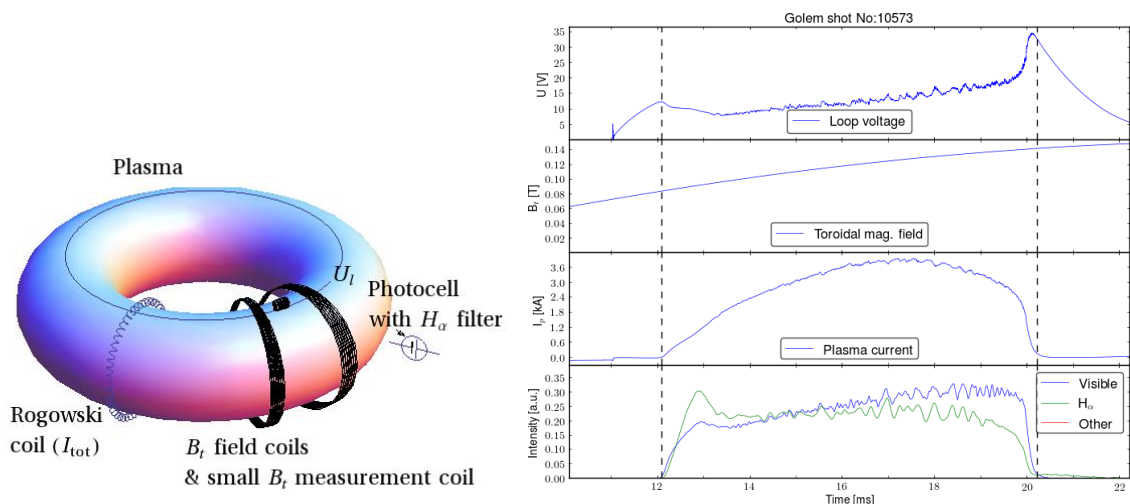
where the resistance of the circuit is equal to $R_C = 5200 \Omega$. Capacitors are charged in time t to desired voltage U_B and once they reach this value, the power source is disconnected. After the triggers are pinned, the capacitors discharge according to the formula

$$U(t) = U_B \exp\left(-\frac{t}{R_C C}\right), \quad (2.9)$$

providing the toroidal coils and plasma current drive by the current I_{TCF} and I_{CD} , which leads to the shot itself.

2.3.2 Diagnostics

The plasma and conditions in the tokamak vessel are monitored by various diagnostics. A few of them are drawn in figure 2.7a. In order to measure the radiation part of the plasma power losses, a photocell is used. It measures the whole spectrum of radiation, but it may be specified by an H_α filter. It shields all frequencies of the EM spectrum except for a narrow gap at the frequency $f = 656.28$ nm. This frequency corresponds to the deep-red visible spectral line in the Balmer series created by hydrogen.



(a) Plasma column and basic diagnostics.

(b) Four basic plots of the analysed data used on the GOLEM tokamak, reprinted from [14].

Figure 2.7: Diagnostics and data analysis on the GOLEM tokamak.

Another diagnostics are used to calculate the effectiveness of the plasma current drive heating, i.e., the resistance R_p of the plasma. To calculate the resistivity of the plasma, knowledge of the plasma current I_p and the voltage in the plasma loop U_l is needed. With knowledge of these variables, Ohm's law

$$R_p = \frac{U_l}{I_p} \quad (2.10)$$

may be used to obtain the plasma resistance.

In order to obtain the plasma current, a Rogowski coil with an integrator is used. A Rogowski coil is a helical coil surrounding the plasma in a poloidal cross-section. It measures the voltage induced in it by the poloidal component of the magnetic field

generated by the plasma current. The output voltage from the Rogowski coil is directly proportional to the derivative of the plasma current flowing through its cross-section. Integration of the measured voltage therefore gives the plasma current I_p itself,[15].

The second variable needed in Ohm's law 2.10 is the toroidal loop voltage U_l . It is the voltage in the plasma generated by the transformer action. This voltage may be thus generated in another single loop of a wire parallel with the plasma column and measured.

Once the discharge is carried out and monitored by the diagnostics, it is necessary to analyse the measured data. Data measured by the mentioned basic diagnostics are plotted in one single graph for comparison and the easier detection of irregularities in the plasma characteristics. An example of plotted results is in figure 2.7b.

But the mentioned diagnostics are only the basic ones used on the GOLEM tokamak. As a small tokamak, GOLEM may have its tokamak chamber opened quite often without a great delay and thus the variance in the used diagnostics is not as big struggle as it is for large tokamaks.

2.3.3 GOLEM strategy

With this easy adaptability, the GOLEM tokamak is a test bed for larger tokamaks. Moreover, this device serves as a test bed for human resources too. For its position as an educational facility is easily accessible by students of the faculty, especially those with a specialisation in Physics and the Technology of Thermonuclear Fusion. Except of its educational purposes GOLEM is a unique experiment in the world due to its internet access. It is possible to access its website and program a pre-set discharge. Once permission is granted by the current supervisor of the tokamak, the queue of the pre-set discharges is carried out. This extraordinary project is already used in remote practical physics courses from other European plasma physics educational programmes. On account of this feature, GOLEM is one of the crucial experiments participating in an international association named FuseNet, The European Fusion Education Network.

The purpose of this association is to unite, coordinate, sponsor and broaden all European plasma physics studies. It represents more than thirty institutions from over fifteen countries. United education necessarily needs communication between individual facilities and because of high cost visits, remote communication and presentations have to be supported. One important way of support for this type of communication is easy accessible virtual models.

Chapter 3

Virtual model

The GOLEM tokamak team has put an effort into such communication support. Such a virtual model was created by O.Pluhar, a graduate of the Faculty of Electrical Engineering of the Czech Technical University, as a bachelor thesis and may be seen at [16]. Although this model has a very good graphical aspect of the work, its usability in presentations diminishes with its dependency on the Windows platform and the necessity of downloading additional Cortona viewer software. This model and its problems set the basic goals of this work and therefore the necessary tools too. One tool, that was not accessible to O.Pluhar and is still partially in development, is WebGL [17], an open graphical library transferred into the web design environment by using the javascript programming language. This library makes it possible to create interactive graphical models accessible as a web site without downloading any software. Moreover, it is supported by all the main web browsers and communication between developers on both sides still widens. Such a variable tool, solving all the problems of previous model, provides many possibilities for the model's appearance and its functions. Therefore, the whole project philosophy had to be set.

As the project had too much potential and thus work to be done, this bachelor thesis could not include the whole project from the idea to a precisely written model and its functions. Hence, the first point of the thesis philosophy was just to demonstrate enormous potential of the model. With every newly developed functionality, show its successful use by one example and withdraw to the creation of another one. The second point arose because of GOLEM's main unique domain, the ability to perform a remotely controlled tokamak operation. As part of work on the remote experiment, the "GOLEM wikipedia" was created and may be seen at [18]. It includes major parameters of the tokamak and reflects the actual setting of the dynamic system. The potential of combining these two projects was obvious, so the second point was set to aim the work in such a direction as to retrieve the needed parameters from the GOLEM wiki and thus achieve the model being up-to-date. As communication with other projects was already part of the work, there was an opportunity to broaden the communication flow to a wide spectrum of software and the third point of the project philosophy was set. The use of the best program in

a particular area should lead to the best results and the modularity of whole project. Therefore anyone can contribute to the improvement of the whole project by simply using a program of his choice and import the results into the model with minor changes in the program source code.

3.1 Programming of online graphics

As philosophy was set, the creation of the model and its functions began. There are many ways to present virtual model, e.g., a game-like application, but a web page was the most elegant solution to problems raised by studying previous work, as mentioned above. On the other hand, the web page method of presentation brought few obstacles. Firstly, the development of internet sites is done with a special set of programming languages.

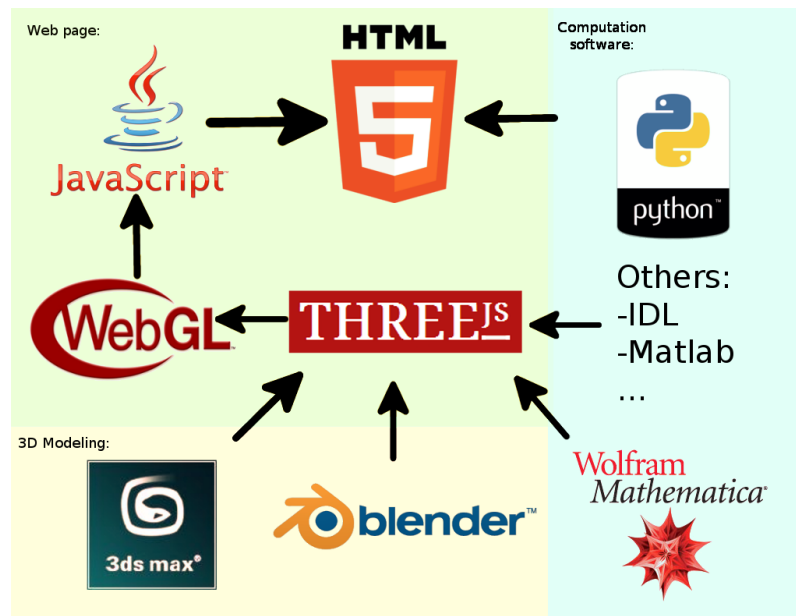


Figure 3.1: Virtual model programming languages and software used in the virtual model alongside arrow-symbolized communication and the hierarchy of individual tools.

The basics of every web page is a standard mark-up language named HTML, Hypertext Mark-up Language. It is the most basic language of web development for it creates individual elements and defines the structure of the whole document. For example a submit button with the label "Send!" is added by the code

```
<button type="submit">Send!</button>.
```

HTML code is stored on a server and sent on request to the user. After this code is received by the user, the web browser uses its display engines to render the site by the given rules on its "canvas". But these graphical engines have their own ways of interpreting basic elements. Therefore, there is a need for a styling language, i.e. CSS. Cascading Style Sheets gives a programmer power over defining how elements will look, e.g., that all bold text has a blue background color setting may be programmed by a simple code

```
.b { background-color: blue; }
```

But HTML provides only a static view of elements without dynamic functionality. In order to make the page dynamic, the developer has to use Javascript. It is embedded into HTML as a labelled script. Therefore, when the browser meets such a label during HTML interpretation, it uses a different engine to compile Javascript functions. The most important difference between HTML and Javascript is that HTML has to reload the whole page with any insignificant change, whereas Javascript provides elements with functions working in runtime. This simple fact was crucial in the formation of the idea to expand the graphics to the internet.

This idea began to be realized in the year 2009 when the Khronos group, a consortium with the purpose of fastening parallel computation. They have started to develop WebGL, an Application Programming Interface (API) providing 3D graphics for web sites. It is based on Javascript, so it runs on the user's side, i.e., places computation tasks on the user's device graphical card, not a server. On the other hand, as WebGL provides a wide range of implements, it becomes hard to develop greater projects without any libraries. Such a library, which makes web 3D graphics simpler, is Three.js. It allows a programmer to add an element by a simple line of code instead of defining each of its vertices, as WebGL would. Adding a cube variable in a scene may be done by the lines

```
var cubeGeometry = new THREE.CubeGeometry( 1, 1, 1 );  
var cubeMaterial = new THREE.MeshLambertMaterial( color: 0xffcd38 );  
var Cube = new THREE.Mesh( cubeGeometry, cubeMaterial );  
scene.add( Cube );
```

In order to create a user friendly virtual model, it is important to use all mentioned languages and libraries (or their equivalents). Not only a virtual model may be achieved this way, but also the whole page environment.

3.2 The environment and other functions of the model

Implementing a user friendly environment is one of the most important parts in programming any presentational software. Not only a wide range of functionalities makes

a virtual model unique, but even more their easy access by the user. In this project a hiding menu on the right edge of the canvas was created for this purpose. The menu on the side was chosen for the fact, that nowadays many monitors have a wide-screen aspect ratio and this aspect ratio would be deepened by a menu on the top or the bottom. Because virtual models are all burdened by a limited entrance due to the limited size of screens, the auto-hiding characteristic of the menu was implemented in order to use as big a part of the browser's canvas as possible. With such access to the model functionalities, it was possible to widen their range.

3.2.1 Project vision

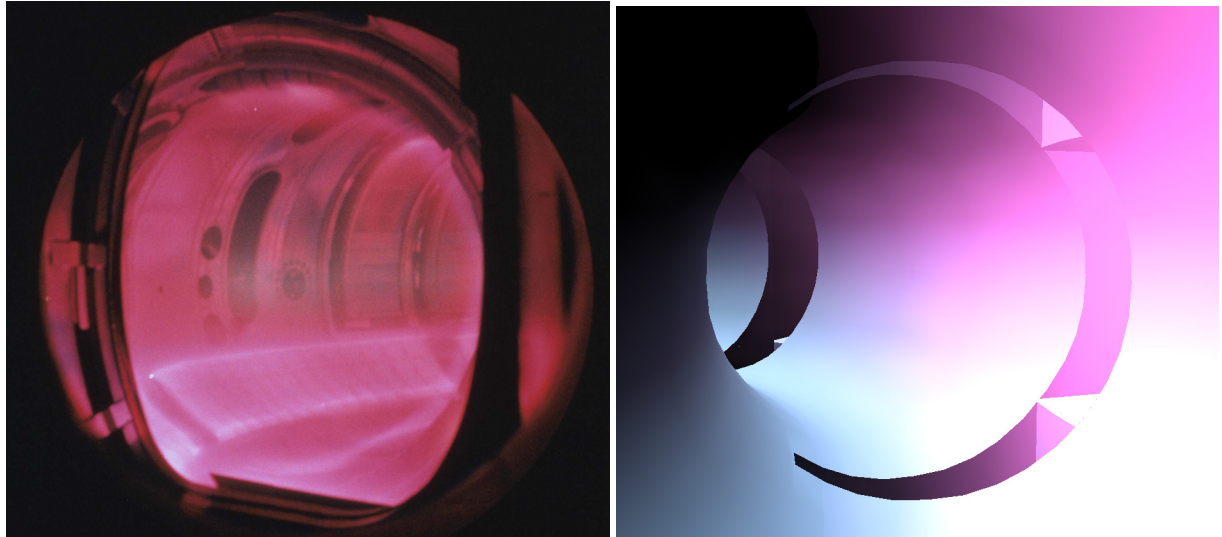
While the basic structure of a project fulfilling the goals of a bachelor thesis were implemented, many ideas and improvements of the project were thought out. Some of them were in the basics, following a philosophy of showing the functionalities with a simple example, implemented above the basic concept of the bachelor thesis (marked by checks on the following list), but it was still impossible to implement all of them. Nevertheless, the horizon of the project was formulated. Roughly categorised, the goals of the project are set as follows:

- ✓ **Create an authentic model of the tokamak room and the infrastructure room.**
- ✓ Display the tokamak by the actual settings on the GOLEM wiki site.
- ✓ Create a simple tool, that would allow the user to switch the visibility of individual objects.
- ✓ Implement basic controls enabling intuitive model exploration.
 - Create a split-screen environment customisable by the user.
 - Implement interaction with individual objects of the model, launching pre-defined sequences visualising the object's functions.
 - Implement a database of registered users, allowing them to save the results of their simulation.
 - Create a tool for the intuitive creation of step-by-step sequences, allowing users to customise a tokamak presentation on their own.
 - To visualise individual technological aspects of a working tokamak in a still state:
 - The vacuum drainage of the tokamak vessel.

- The purification of the tokamak vessel, including glow discharge and chamber baking.
- Display individual technological aspects of a working tokamak in a preparation phase:
 - ✓ **The charging process of the tokamak capacitor banks for the toroidal magnetic field coils.**
 - The charging process of the tokamak capacitor banks for the current drive winding.
 - The charging process of the tokamak capacitor banks for the breakdown winding.
 - Filling the tokamak vessel with the working gas.
- Visualise individual technological aspects of a working tokamak during the discharge:
 - Triggering the discharge of capacitor banks to the corresponding coils.
- Visualise individual physical aspects of a working tokamak during the discharge:
 - The discharge process of the tokamak capacitor banks for the toroidal magnetic field coils, the current drive winding and the breakdown winding.
 - ✓ **The toroidal magnetic field B_t .**
 - The toroidal electric field E_{CD} generated by the current drive winding.
 - The toroidal electric field E_{BD} generated by the breakdown winding.
 - The horizontal and vertical magnetic field of stabilisation.
 - ✓ **Plasma.**
 - The magnetic flux in the transformer core.
 - The pre-ionisation from both the electron gun and electromagnetic waves.
 - The function of all diagnostics.
- Display individual physical aspects of a working tokamak after the discharge:
 - The short-circuiting of the capacitor banks.
 - Data analysis by computation nodes.
 - The presentation of discharge data in a page environment.

All bold-text points correspond to the main goals of the bachelor thesis and were part of the basic structure implementation. Their descriptions are in chapters 3.1:Programming of online graphics, 3.3:Capacitor curve and 3.4:Models of the toroidal magnetic field B_t except for plasma creation.

It is not explicitly listed in the thesis goals, but the creation of the model of tokamak includes the plasma too. In order to visualise a trustworthy plasma ring, it was necessary to use the low level method of WebGL described above. By using shaders, two models of the plasma were created. The first one is static and was designed to look like real hydrogen plasma captured in photographs.



(a) Hydrogen plasma captured on the TEXTOR tokamak, reprinted from [19]. (b) Plasma column displayed by a static model created by WebGL.

Figure 3.2: Comparison of the plasma model and the photography of hydrogen plasma captured on the TEXTOR tokamak.

The second one is not as authentic as the first one in its appearance, instead it is focused on the dynamic visualisation of plasma. It was achieved by a few steps beginning with toning the colors of the lava texture. Afterwards, with the model loading, this altered texture is loaded twice on the same surface, and are blended dynamically. To achieve the global noise given by the plasma bumping, the basic texture of clouds was used. When textures are loaded, bump mapping, a technique to create an illusion of surface irregularities, was used. The result is provided in figure 3.3.

Except of the basic concept, few other functionalities were implemented. They focus on displaying the tokamak in various settings and from different views. Basics of such functionality are controls allowing movement through the model itself. Monitoring keyboard events and capturing mouse movement over the canvas of the browser may be recalculated as a camera movement and its rotation. In this way, one type of accessible control modes

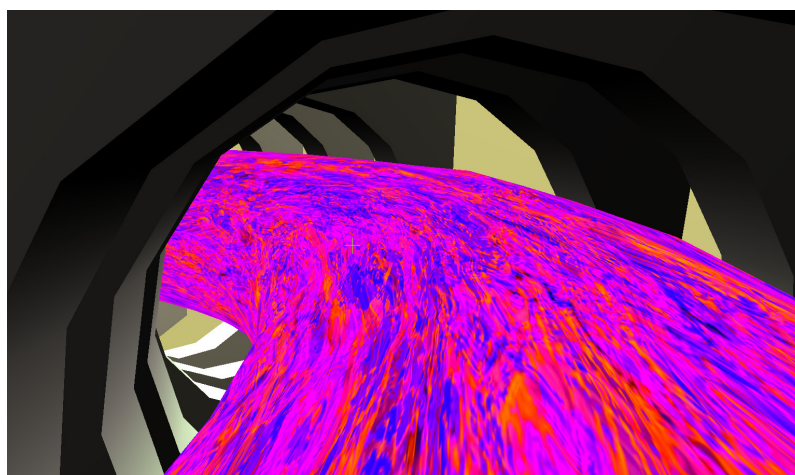


Figure 3.3: Plasma column visualisation by bumping model.

is implemented and its coefficients of movement recalculation are small, so the movement is slow enough and user may explore all components of tokamak in detail, e.g., position camera to the middle of plasma column. On the other hand, second control mode is more realistic, simulating presence in the tokamak room by gravity engine.

When the camera positioning is solved, variability of the vision is the next struggle. As tokamak has many individual components it often becomes confusing. Therefore, all meshes imported in the model has its own visibility switch in the options tab of the menu. By turning off desired parts of tokamak, user may customize the model by his own will.

But main tokamak parts are not the only things, that are imported to the model. Diagnostics database is imported as well and situated on default positions. These positions may be changed by selecting another position in drop-down element, which is located in options tab of the menu. The default positions are meant to be loaded from GOLEM wiki page as well and thus be actual by every reload of the page.

This communication with GOLEM wiki is already implemented in the example of capacity of capacitor banks. As page loads, request is sent on the server, where it retrieves the value of actual capacity. This value is used in the physical kernel (functions calculating real physical problem), simulating physical conditions before and during the discharge.

This kernel fulfils the stated goals of work and follows its philosophy. To create and present only a simple example of a possible function and create a modular environment prepared to be extended by any contributor. Most general physical models were created in order to show how these simulation programs are attached to the web site.

The physical kernel behind the model may be divided in two main domains. The first works in runtime, reacting to the user's actions. The second is too computationally

demanding to be finished in the time scale of the user's visit.

3.3 Capacitor curve

The first domain is in the model represented by a charging curve of the capacitors, whose physics was already described in chapter 2.3.1: Setup.

As all physical variables except for the desired voltage in equation 2.8 are fixed, input form for this task basically consists of one select element. Other constants are given or gathered from the tokamak's wikipedia, so they remain actual in the case of any power supply parameter changes. Once all variables are known, the requested values are submitted, which means that a request is created and passed to a script on the server. As the script is executed, it creates a file, reflecting the time development of the capacitor voltage with a pre-defined time step. As soon as execution ends, a message with the file location is sent back to the web page, which retrieves these data to display them.

This part is done with the use of the Javascript library Dygraphs.js. It creates a user friendly environment, which allows an easy examination of the desired part of the data set. For future development it should be noted that the library is specialised in plotting huge data sets, and may therefore one day serve for the comparison of a numerical model with data sets measured by the diagnostics of the tokamak.

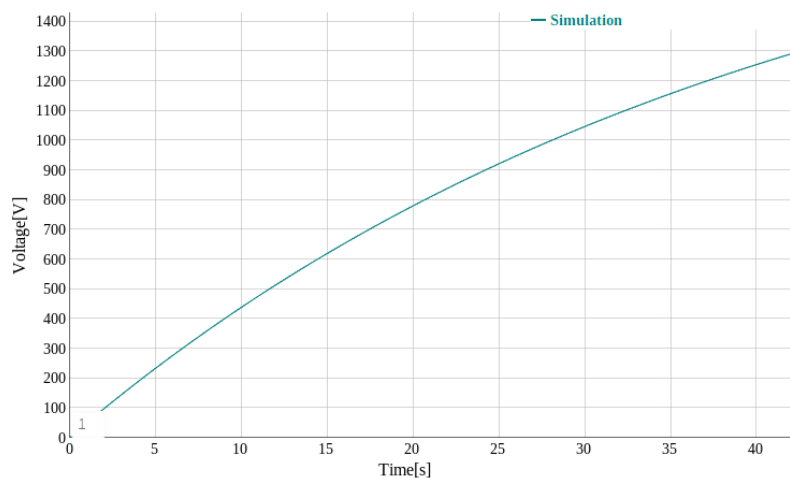


Figure 3.4: Charging of the capacitors curve in a Dygraphs.js environment.

An experiment was carried out to confirm the results of the simulation script. With six B_t capacitor banks of overall capacity $C_B = 67.5$ mF and resistance of circuit $R_C = 5220 \Omega$, capacitors voltage was measured in time as well as supply voltage. Ideally, the supply

voltage would be constant, but as power source with high inner resistance is used at GOLEM tokamak, its supply voltage changes with rising voltage in capacitors. With initial voltage of $U_i = 850$ V and final voltage of $U_f = 1050$ V, average of these values $U_a = 950$ V was taken as a constant value in simulation. The simulation results are shown in the figure 3.5 as well as the experiment data. The equation 2.8 shows that with a higher supply voltage, the capacitor voltage rises faster. This fact is confirmed by the experiment, as the capacitor voltage overreaches the simulation values as it approaches final value of the supply voltage U_f .

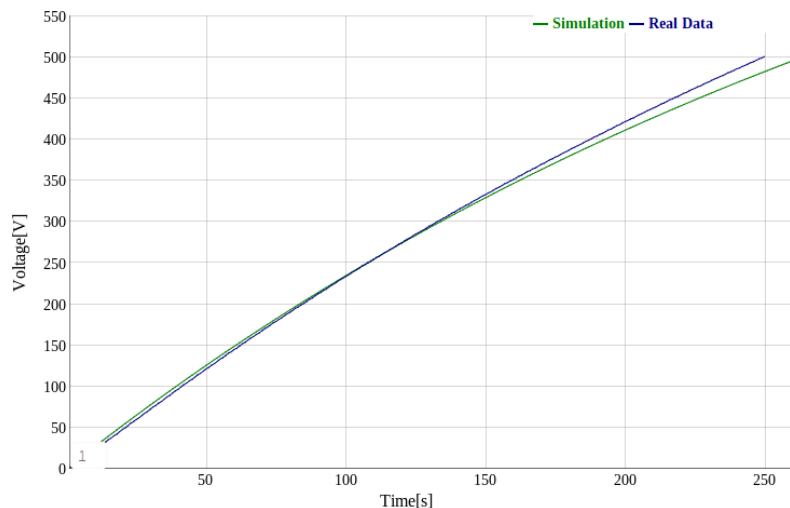


Figure 3.5: The comparison of simulation and experiment results.

3.4 Models of the toroidal magnetic field B_t

As mentioned earlier, not every model may be calculated in runtime and needs to be pre-calculated by high performance computational devices or clusters. Software specialized in such tasks is Wolfram Mathematica, Matlab or IDL, but a wide spectrum of programs may be used. The only condition imposed on the program is a suitable output, e.g., a graphical model. This data may be imported by web page and in the case of a graphical model added to the scene as a mesh.

This particular case was used in this work by exporting a graphical model of the toroidal magnetic field within the vessel from Wolfram Mathematica and is accessible through the options tab of the menu. Mathematica computations consisted of the creation of a grid, as the numerical model needed to be finitely differentiated, and physical calculations. The grid may have been chosen equidistant in Cartesian coordinates, but

more convenient was the use of cylindrical coordinates for the axis symmetry of the tokamak as mentioned in chapter 2.2: Toroidal magnetic field \mathbf{B}_t . By such easement, it was necessary to calculate the contribution from only one coil. This partial result may then be copied afterwards and rotated around the tokamak axis for each coil. By the superposition of all grids, a complete result is achieved. It shows the homogeneity of the toroidal magnetic field expected from a continuous solenoid model, but in addition visualises the ripple of field dependent on magnetic field coils positions and orientations. It reflects the positions of the coils by a stronger field and gaps between them with the lower field.

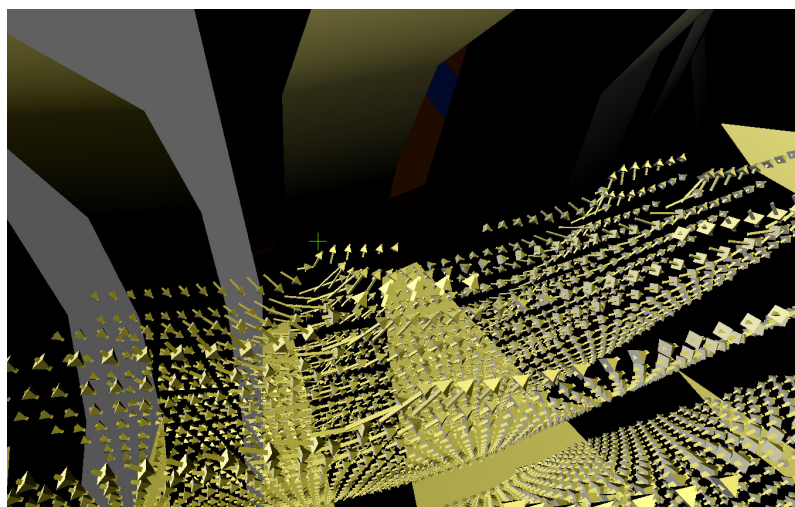


Figure 3.6: The ripple of the toroidal magnetic field by the vessel wall.

As long as ports are considered, the displacement of the coils from the original grid given by cylindrical coordinates appears. This problem may be solved by well chosen parameters of the grid and by adding a calculation for a few of the displaced coils. By copying these coils contributions and their addition may be calculated the whole toroidal magnetic field B_t with precise results by the ports, where the coils are displaced from the original equidistant model.

On the other hand, the grid has to be dense enough to display ripple by the coils and such a dense grid is unnecessary in the homogeneous part of the field. Some adjustments may be done by a different density of grid, but such a model intuitively suggests a lesser intensity of the toroidal magnetic field in the homogeneous part. Therefore, for the usual purpose of describing the basic characteristics of a toroidal magnetic field, another model was created with a much sparser grid of points. It follows the physics described earlier and shows the dependency of $B_t \sim R^{-1}$. Moreover, it shows the simplicity of the addition

of a new model for potential contributors.

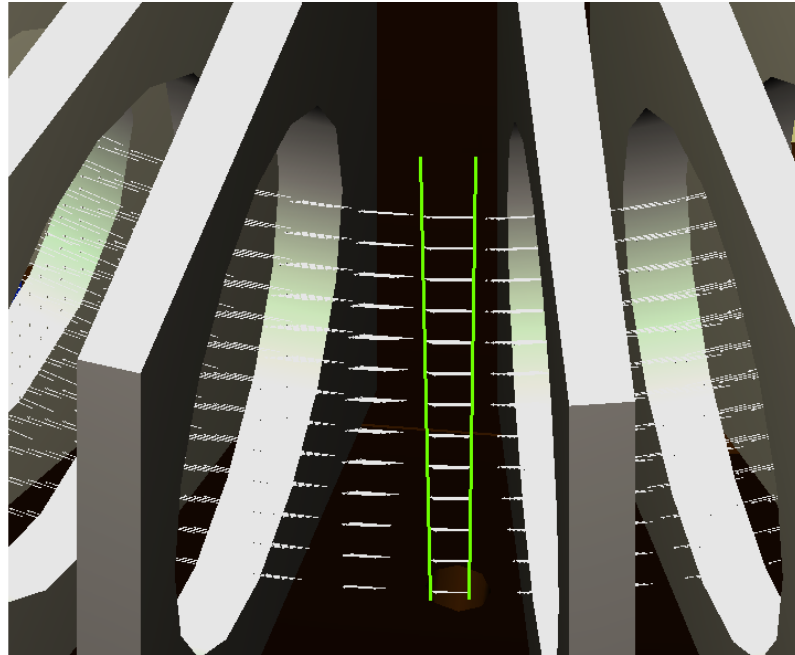


Figure 3.7: The dependency of $B_t \sim R^{-1}$ with a drop in the intensity of the toroidal magnetic field by $2/5$ from the high field side to the low field side.

As a vector field was described in both cases, it was necessary to decide how to visualise the data sets. There are three usual methods of vector field visualisation.

- The first works with particles, showing their flow in the field. It is widely used to describe problems, where the field influences particles by accelerating them in the direction of the vector field in their positions. However, the magnetic field influences particles over the vector product and therefore this approach would be too computationally demanding.
- The second type describes the vector direction by a normalised arrow and its intensity by colour. This model may be used in most cases, but is not as synoptic as the last model.
- The last model differs from the second one by the description of vector magnitude as arrow length. Although it may be confusing in many vector field descriptions, both the mentioned models gave the best results when this visualisation of the vector field was used. Results given by this approach may be seen in figures 3.6 and 3.7.

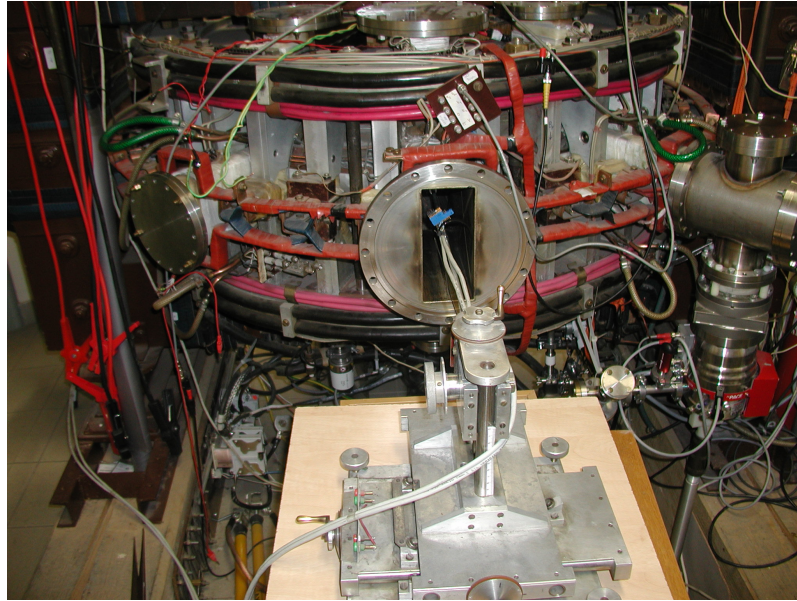


Figure 3.8: Hall probe position at the GOLEM tokamak.

In order to confirm the model based on Biot-Savart law, values of toroidal magnetic field B_t from simulation were compared to the data set measured by the hall probe, diagnostic used to measure toroidal magnetic field by the use of Hall effect. Its position during the measurement is shown in figure 3.8. The probe is described in more detail in [20]. The comparison of both data sets is shown in the figure 3.9.

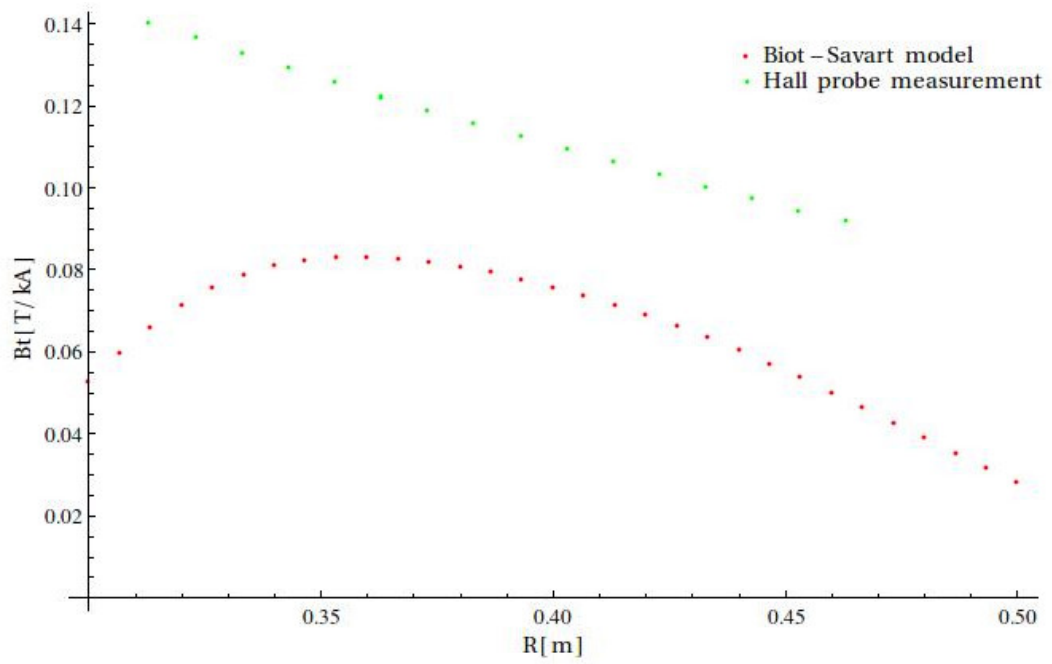


Figure 3.9: The comparison of data sets from the simulation and the experiment carried out in [20].

Summary

This thesis documents an online virtual model created with a purpose of presentation of GOLEM tokamak. Placing 3D graphics model online was achieved by a library WebGL supported by all main internet browsers. Because of physical aspect of tokamak device, basics of tokamak physics were implemented to the graphical model.

Two physical simulations of toroidal magnetic field were made. First uses knowledge of decrease in the magnitude of the toroidal magnetic field with inverse dependency on of-axis radius R . The second one is based on a fundamental law of physics, Biot-Savart law. This model was compared with the measurements on GOLEM tokamak, but data sets did not match. Most significant difference were by the toroidal coils, as the ripple of the toroidal magnetic field is more significant in the simulation than in the reality. This is probably caused by other sources of the toroidal magnetic field, e.g. chamber current I_{ch} .

Another simulation is more connected with the web interface, responding on user's actions in runtime. It calculates capacitor bank charging and displays the result in the interface. Results of this simulation were compared with real measurements too. In this case, the two data sets correspond very well, with deviations caused by the imperfection of the supply power source.

Bibliography

- [1] Nuclide Stability. *University of Waterloo* [online]. ©1992-2014 [cit. 2014-07-21]. Available at: <http://www.science.uwaterloo.ca/~cchieh/cact/nuctek/nuclideunstable.html>
- [2] STEFANO ATZENI, Jürgen Meyer-ter-Vehn. *The physics of inertial fusion beam plasma interaction, hydrodynamics, hot dense matter*. Oxford: Clarendon Press, 2004. ISBN 01-915-2405-0.
- [3] CHEN, Francis F. *Úvod do fyziky plazmatu*. 1. vyd. Praha: Academia, 1984, 328 s.
- [4] Plazmak2010 [ONLINE]. Available at: <http://www.szfki.hu/images/lphys/plazmak2010.jpg> [Accessed 2014-07-21].
- [5] LIBRA, Martin, Jan MLYNÁŘ a Vladislav POULEK. *Jaderná energie*. 1. vyd. Praha: Ilsa, 2012, 167 s. ISBN 978-80-904311-6-4.
- [6] SHAFRANOV, Vitalii D. The initial period in the history of nuclear fusion research at the Kurchatov Institute. *Physics-Uspekhi* [online]. 2001-08-31, vol. 44, issue 8, s. 835-843 [cit. 2014-07-20]. DOI: 10.1070/PU2001v044n08ABEH001068. Available at: <http://stacks.iop.org/1063-7869/44/i=8/a=A13?key=crossref.719505968875b4c998f5b61b3d9b64d5>
- [7] Stellarators [ONLINE]. Available at: <http://www.efda.org/wpcms/wp-content/uploads/2011/11/stellarators-e1322663145672.jpg> [Accessed 2014-07-21].
- [8] Physical principle of tokamaks. *GOLEM@FJFI.CVUT* [online]. ©2008 [cit. 2014-07-20]. Available at: http://golem.fjfi.cvut.cz/?p=documentation_tokamak_overall
- [9] Anwendung: Driften in ringförmigen Magnetfeldern [ONLINE]. Available at: http://images.slideplayer.de/7/1784310/slides/slide_26.jpg [Accessed 2014-07-21].
- [10] BROTKÁNKOVÁ, Jana. *Study of high temperature plasma in tokamak-like experimental devices*. Prague, 2009. Available at:

<http://golem.fjfi.cvut.cz/wiki/Library/GOLEM/PhDthesis/JanaBrotankovaPhDthesis.pdf>.
Dissertation. Faculty of Mathematics and Physics, Charles University in Prague.

- [11] Biot-Savart law [ONLINE]. Available at:
<http://hyperphysics.phy-astr.gsu.edu/hbase/magnetic/imgmag/bsav.gif> [Accessed 2014-07-21].
- [12] The past modifications and history of the device. *GOLEM@FJFI.CVUT* [online]. ©2008 [cit. 2014-07-20]. Available at:
http://golem.fjfi.cvut.cz/?p=documentation_history
- [13] Tokamak GOLEM: Characteristics. *GOLEM@FJFI.CVUT* [online]. ©2008 [cit. 2014-07-21]. Available at: <http://golem.fjfi.cvut.cz/?p=tokamak>
- [14] Tokamak GOLEM: Shot database. *GOLEM@FJFI.CVUT* [online]. 10.01.2013 [cit. 2014-07-21]. Available at: <http://golem.fjfi.cvut.cz/shots/10573/>
- [15] ĎURAN, Ivan. *Fluctuations of magnetic field in the CASTOR tokamak*. Prague, 2003. Available at:
<http://golem.fjfi.cvut.cz/wiki/Library/GOLEM/PhDthesis/IvanDuranPhdThesis.pdf>.
Dissertation. Faculty of Mathematics and Physics, Charles University in Prague.
- [16] PLUHARŮ, Ondřej. Virtual model of GOLEM tokamak. *GOLEM@FJFI.CVUT* [online]. ©2008 [cit. 2014-07-20]. Available at: <http://golem.fjfi.cvut.cz/virtual/>
- [17] WebGL: OpenGL ES 2.0 for the Web. *The Khronos Group Inc.* [online]. ©2014 [cit. 2014-07-20]. Available at: <http://www.khronos.org/webgl/>
- [18] GOLEM wiki. *GOLEM@FJFI.CVUT* [online]. ©2008 [cit. 2014-07-20]. Available at:
<http://golem.fjfi.cvut.cz/wiki/>
- [19] The Trilateral Euregio Cluster. VAN EESTER, Dirk. *ITER and Fusion Energy* [online]. [cit. 2014-07-21]. Available at: <http://iter.rma.ac.be/en/community/TEC/>
- [20] MARKOVIČ, Tomáš. *Measurement of Magnetic Fields on GOLEM Tokamak*. Prague, 2012. Available at:
<http://golem.fjfi.cvut.cz/wiki/Library/GOLEM/MastThesis/MarkovicTomas.pdf>.
Diploma thesis. Faculty of Nuclear Sciences and Physical Engineering, Czech Technical University in Prague.

Appendix

Appendix A

Table of variables

Variable	Basic unit	Name
E	[J]	Energy
Δm	[kg]	Mass difference
σ	[barn]	Nuclear cross-section
v_r	[ms ⁻¹]	Relative velocity
μ	[kg]	Reduced mass
Z	[-]	Proton number
T	[eV]	Temperature
Δ	[m]	Width of electron layer
E_k	[J]	Kinetic energy
U_p	[V]	Potential voltage
E	[Vm ⁻¹]	Electric field
n_e	[m ⁻³]	Electron density
λ_D	[m]	Debye length
T_e	[eV]	Electron temperature
L	[m]	Size of described system
ω_{pe}	[s ⁻¹]	Plasma electron frequency
τ_{col}	[s]	Average time between collisions of particle with neutral particle
N_D	[-]	Plasma parameter
τ_E	[s]	Confinement time
W_P	[J]	Plasma energy
P_L	[W]	Plasma power losses
P_H	[W]	Heat power
P_e	[W]	External heat power
P_i	[W]	Internal heat power
Q	[-]	Fusion gain
V_p	[m ³]	Plasma volume

Variable	Basic unit	Name
ε_f	[-]	Energy gain from one reaction
R_V	$[\text{s}^{-1}\text{m}^{-3}]$	Rate of fusion reactions in plasma volume
n_D	$[\text{m}^{-3}]$	Density of deuterium fuel
n_T	$[\text{m}^{-3}]$	Density of tritium fuel
N_p	[-]	Number of particles
n	$[\text{m}^{-3}]$	Density of particles
B_t	[T]	Toroidal component of the magnetic field
B_p	[T]	Poloidal component of the magnetic field
B	[T]	Complex magnetic field inside a tokamak chamber
F_L	[N]	Lorentz force
v	$[\text{ms}^{-1}]$	Velocity of a particle
q	[C]	Charge of a particle
E_d	$[\text{Vm}^{-1}]$	Drift electric field
ε_{ind}	[V]	Induced voltage in a circuit
Φ_{tor}	[Wb]	Magnetic flux through the area enclosed by plasma ring
B_{tor}	[T]	Magnetic induction in the area enclosed by plasma ring
S_{tor}	$[\text{m}^2]$	The area enclosed by plasma ring
j	$[\text{Am}^{-2}]$	Current density
R	[m]	Radius from the tokamak axis
I	[A]	Electric current
I_{TCF}	[A]	Electric current in the toroidal field coils
r	[m]	Radius
r_0	[m]	Vessel minor radius
R_0	[m]	Vessel major radius
N	[-]	Number of coils
I_p	[A]	Plasma current
C_B	[F]	Capacitance of the B_t capacitor bank
τ	[s]	Discharge length
C_G	[F]	Capacitance of all capacitor banks on GOLEM tokamak
ε	[V]	Supply voltage
R_C	$[\Omega]$	Resistance of the charging circuit
C	[F]	Capacitance of capacitor banks
U_B	[V]	Desired voltage for C_B capacitor bank
t	[s]	Time
I_{CD}	[A]	Current in the major primary coil of the transformer
f	$[\text{s}^{-1}]$	Electromagnetic spectrum frequency
R_p	$[\Omega]$	Plasma resistivity

U_l	[V]	Loop Voltage measured a wire loop arround the tokamak
E_{CD}	[Vm ⁻¹]	The toroidal electric field generated by the current drive winding
E_{BD}	[Vm ⁻¹]	The toroidal electric field generated by the breakdown winding
U_i	[V]	Initial value of supply voltage
U_f	[V]	Final value of supply voltage
U_a	[V]	Average value of supply voltage
I_{ch}	[A]	Current driven through the conducting chamber

Table of constants

Variable	Approximate value	Name
π	3.1415926	Pi
c	299792458 ms ⁻¹	Speed of light
\hbar	1.0545717×10 ⁻³⁴ Js	Reduced Planck constant
e	1.6021765×10 ⁻¹⁹ C	Electron charge
m_e	9.1093829×10 ⁻³¹ kg	Electron mass
ϵ_0	8.8541878×10 ⁻¹² Fm ⁻¹	Vacuum permittivity
μ_0	1.2566370×10 ⁻⁶ VsA ⁻¹ m ⁻¹	Vacuum permeability
k_B	1.3806488×10 ⁻²³ JK ⁻¹	Boltzmann constant